Research Square

Preprints are preliminary reports that have not undergone peer review.
They should not be considered conclusive, used to inform clinical practice,
or referenced by the media as validated information.

From milling to herding: aggression-driven transition toward low-energy ordered states

Flora Grilli

flora25@mit.edu

Massachusetts Institute of Technology

Grgur Tokić

Massachusetts Institute of Technology

Dick K.P. Yue

Massachusetts Institute of Technology

Article

Keywords: Collective behavior, Aggressive behavior, Swarming dynamics, fish aquaculture

Posted Date: November 17th, 2026

DOI: https://doi.org/10.21203/rs.3.rs-11433894/v1

License: This work is licensed under a Creative Commons Attribution 4.0 International License.
Read Full License

Additional Declarations: No competing interests reported.

From milling to herding: aggression-driven transition toward low-energy ordered states

Flora Grilli[1*], Grgur Tokić[1] and Dick K. P. Yue[1]

[1]Department of Mechanical Engineering, Massachusetts Institute of Technology, 77 Massachusetts Ave, Cambridge, 02139, MA, USA.

*Corresponding author(s). E-mail(s): flora25@mit.edu;
Contributing authors: gtokic@mit.edu; yue@mit.edu;

Abstract

Collective behavior studies how large-scale coordination emerges in groups of individuals, such as animals, that only perceive their immediate neighbors. Analytic models of collective motion predominantly describe homogeneous swarms; in such swarms, large coherent patterns like mills are known to emerge. Among animals, however, inter- and intra-species heterogeneous behavior is ubiquitous. Importantly, the effect of animal-like heterogeneous aggression on the collective states of swarms is not well understood. Here, we introduce novel heterogeneous rules in a Vicsek-like swarming model to simulate unsteady, animal-like aggressive behavior among self-propelled agents. We find that milling behavior becomes unstable to aggression, and that an aggression-driven transition exists between newly identified steady collective states. Mill destruction and herding are new transition mechanisms propelling the transition from milling to flocking and flocking to banding. Despite aggression being present, the new ordered phases in the swarm are relatively energetically inexpensive. Additionally, we find that swarm welfare deteriorates with density. This is the first time that the effect of aggressive behavior on large swarms has been modeled analytically. The newly defined behavioral rules are inspired by aggressive behavior in fish, but are broadly applicable to agonistic behavior in animal groups.

Keywords: Collective behavior, Aggressive behavior, Swarming dynamics, fish aquaculture

1 Introduction

Collective behavior describes the large scale coordinated movement of groups of individuals. It is present in nature across many species, such as bacteria, insects, fish, birds, some quadrupeds and even humans [1–4]. The study of collective motion continues to fascinate the scientific world, as large cohesive patterns emerge at the group level even when each individual can only perceive its immediate neighbors [1–4].

In homogeneous swarms, the emergent collective patterns are relatively well studied. In the animal world, large global collective patterns ranging from flocks of starlings to compact, swirling, ball-like mills of herrings (bait balls) emerge from short-range interactions among immediate neighbors [5]. In particular, the complex collective patterns of schooling fish have been extensively researched using analytical methods [6–8], experimental approaches [9, 10], deep learning [11], and hydrodynamics [12, 13].

Despite extensive research on homogeneous collective behavior, the effects of heterogeneous behavior on swarm dynamics and energetics remain less well-understood. Complex heterogeneous behavior within collectives is present in nature in diverse cases [14]. For example, coordination can arise from interaction between interspecific heterogeneous groups, such as a wolf pack hunting prey [15], and shepherding dogs herding a flock of sheep [16]. Intraspecific heterogeneous interaction can also lead to collective phenomena such as leader-follower behavior within a flock of sheep [17], variation in locomotory states (stationary, walking, hopping) in groups of locusts due to anisotropic neighbor distributions [18], and vast swarming patterns in locusts arising in part from individuals exhibiting cannibalistic or escape behaviors [19, 20]. In all of these cases, large scale coordinated movement can emerge from local heterogeneous interactions.

Aggression among fish is another example of intraspecific heterogeneous behavior commonly found in nature as well as in aquaculture; it is typically driven by competition over resources or by social hierarchy [21–23]. Fin-fish aquaculture is rapidly developing and intensifying to meet the global demand for protein [24]; however, the confined, high-density environment in aquaculture presents new challenges for the study of fish school behavior [25]. In particular, the ubiquitous presence of aggression in aquaculture leads to chronic stress, disparate growth rates, fin loss, and disease [21–23]. The overcrowding of fish in aquaculture is related to the extensive use of antibiotics in fish farms [26, 27], which is reflective of poor fish welfare and poses health risks to the consumer. Combined, these factors reduce the quality and quantity of fish stock [28], resulting in economic loss and poor fish welfare conditions [23].

Computational models are key tools that help to elucidate the collective behaviors of animal-like groups. Collective behavior in homogeneous swarms is well captured with analytic models of self-propelled agents moving at steady speed that interact only with a finite number of their immediate neighbors [29–32]. In the foundational Vicsek model [29], each agent finds neighbors within a limited interaction radius at discrete decision times and updates its own heading based on its neighbors' headings. Using only this alignment rule, ordered motion emerges as density increases and noise decreases [1, 29]. The minimal milling model [33] captures milling behavior (rotation about a common center) remarkably well by constraining the turning rate and field of view of agents in a Vicsek-like model. Similarly, introducing repulsion (which enforces

personal space) and attraction (which enables cohesion) along with alignment leads to more complex patterns of collective behavior [30].

In contrast to homogeneous swarms, the modeling of heterogeneous swarms and heterogeneous behavior is far less developed. While some models incorporate heterogeneity in speed [34, 35], dynamics and time-delay [36, 37], and field of view [38], comparatively few investigate the effects of behavioral heterogeneity (i.e., within-group differences in behavioral rules) [39–41]. The "group chase and escape" model [41], an extension of the classical "chases and escapes" mathematics problem, represents a binary mixture of agents where one group chases the other until all escapees are captured. In this case, each chaser acts to move towards the nearest escapee, while each escapee acts to move away from the nearest chaser. This is similar to the modeling of wolf-pack hunting [15] or the shepherding problem [16] where individuals follow de-centralized neighbor-informed behavioral rules until a goal is achieved, such as capture of the prey or shepherding the flock to a desired area. However, since the goal of the group chases and escapes model [41] is capture, the long-term steady-state behavior of a heterogeneous swarm is not characterized. Conversely, del Mar Delgado et al. [40] introduce behavioral heterogeneity in a swarm by applying different strengths to alignment and attraction behavior without any target outcome. Similarly, Copenhagen et al. [39] introduce behavioral heterogeneity to a swarm by non-alignment, both as a binary mixture with a fraction of non-aligners and as a spectrum of non-alignment behavior. With this model, coordination is inhibited in some cases, while in other cases, aligners self-sort away from non-aligners [39]. Though the collective patterns of a swarm with heterogeneous behaviors is captured, non-alignment is not representative of aggressive behavior in animals.

In this work, we introduce novel heterogeneous behavioral rules in a Vicsek-like model to simulate unsteady and aggressive behavior in large swarms of binary populations (aggressive and non-aggressive agents). These aggression-inspired heterogeneous behavior rules also induce temporal speed variability of agents in the swarm. Using extensive computational simulations, we show that aggression drives a transition between the steady-state collective behaviors of the swarm. Notably, mill destruction causes a transition from steady milling to a stable polarized flocking state in low-aggressive swarms, while herding in a high-aggressive swarm causes a transition from stable polarized flocking to a quasi-steady banded state. We evaluate the relative energy cost and rate of "bites" in the swarm, and find that they are non-monotonically related to aggression level, but correlated with swarm density. Despite aggression being present, the new behavioral phases in the swarm are relatively energetically inexpensive.

The newly defined aggression rules are inspired by aggressive behavior in fish; however, they are broadly applicable to any animal group displaying agonistic behavior. In fact, the patterns of collective behavior resulting from our model are suggestive of behaviors found in nature, such as in schools of fish, herds of sheep, and swarms of locusts (see Figure 1). To our knowledge, this is the first time aggressive, heterogeneous behavior has been introduced to a Vicsek-like swarming model.

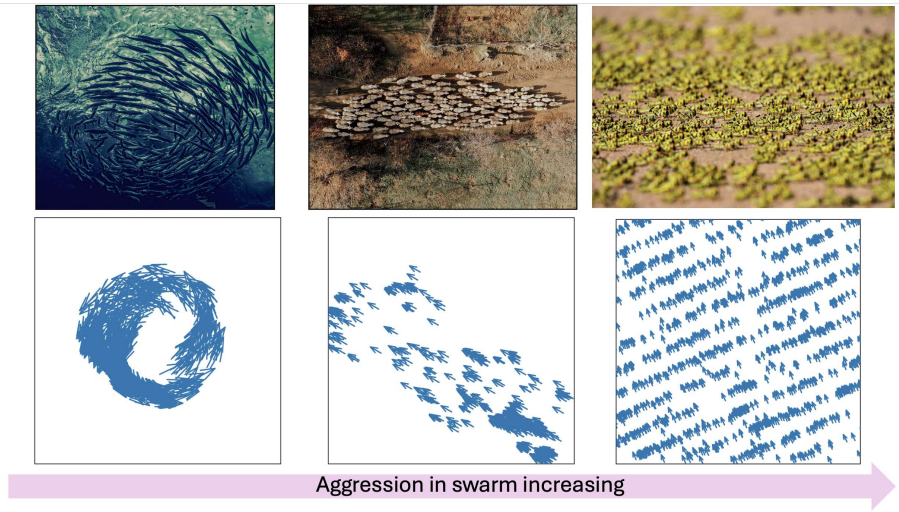


Fig. 1 As aggression increases in a swarm, the steady-state collective behavior resulting from our simulations changes (*bottom row*), capturing qualitative similarities with animal groups (*top row*): a fish bait ball (*left*; Credit: Isabel Fowler), a flock of sheep (*center*; Credit: Emin Alper), and marching bands of locusts (*right*; ©FAO/Michael Tewelde).

2 Aggressive behavior model

We introduce novel heterogeneous behavioral rules in a Vicsek-like swarming model to simulate unsteady animal-like aggression. A Vicsek-like model simulates self-propelled agents that respond to interactions within a finite neighborhood. In Section 2.1, we describe the motivation and background behind the new behavioral rules, while in Section 2.2, we formally define the model parameters. In Section 2.3, we describe the rules governing the model, and in Section 2.4 we define quantitative metrics for aggression.

2.1 Animal-like aggression

We develop novel behavioral rules that are inspired by aggressive behavior within animal groups, such as fish. Aggression among fish is often linked to social hierarchy. In such groups, strong dominant fish are aggressive towards weaker submissive fish by performing bites, chases, and attacks [21, 23]. Here, we represent dominant and submissive individuals with a binary population of aggressive and non-aggressive agents, and we define events that represent a bite, a chase maneuver and an escape maneuver.

Attacks and bites in groups of fish are often triggered by territoriality [21], so we define the rules such that aggression is triggered by proximity, i.e., within a limited space around an aggressive individual. As fish tend to burst in fast accelerations, we introduce unsteady behavior via the burst speed, which is used in our model in a chase or escape. We assume the burst speed ratio (burst speed to steady speed) to be greater than one; from data, the burst speed ratio in fish can be as big as ~ 10 [42].

While the aggression rules are inspired by known fish behavior, they remain general to agonistic behavior in other groups of animals, or even in swarms of robots and drones. In Figure 1, we show qualitative similarities between our simulations and groups of fish, sheep, and locusts.

2.2 Model parameters

In this study, heterogeneous behavior is introduced to an otherwise homogeneous Vicsek-like model. A swarm $\mathscr{S}$ of size $N = |\mathscr{S}|$ and density ρ is simulated in a square domain with doubly periodic boundary conditions, where each agent, $\mathcal{A}_i$, is initiated with randomly distributed positions and headings, and steady speed v_s. At any time t, the state of each agent is given by $\mathcal{S}_i(t) = \mathcal{S}(\boldsymbol{x}_i(t), \boldsymbol{h}_i(t); v_i(t))$, where the index $i \in [1, N]$ uniquely defines each agent in the swarm, and $\boldsymbol{x}_i(t)$, $\boldsymbol{h}_i(t)$, $v_i(t)$ denote the position, heading, and speed of an agent, respectively.

The homogeneous model follows a simple alignment rule: at each decision time t_j, each agent acts to align with the headings of its neighbors, constrained by the maximal turning rate ω. The neighbors to $\mathcal{A}_i$ are found within the field of view, $\mathcal{F}_{v,i} = \mathcal{F}_v(r, \phi; \boldsymbol{h}_i(t))$ — a circular sector confined by the interaction length r and the view angle ϕ, and bisected by the heading $\boldsymbol{h}_i(t)$. The position of each agent is updated kinematically as,

$$\boldsymbol{x}_i(t_{j+1}) = \boldsymbol{x}_i(t_j) + v_i(t_{j+1})\boldsymbol{h}_i(t_{j+1})\delta t, \tag{1}$$

where $t_{j+1} = t_j + \delta t$, and the discrete timestep, δt, models the reaction time of an agent in the swarm. (For notational simplicity, we hereafter omit time-dependent notation, reintroducing it only where required for clarity.) Further information on the homogeneous model is located in the Methods section (Section 5.1).

To introduce heterogeneous aggression, we define a binary population composed of an aggressive subpopulation, $\mathscr{A}$, and a non-aggressive subpopulation, $\mathscr{B}$. Aggressive agents A_i are members of $\mathscr{A}$ and non-aggressive agents B_i are members of $\mathscr{B}$. The notation for an agent $\mathcal{A}_i$ refers to any arbitrary agent in the swarm $\mathscr{S}$, whether a member of $\mathscr{A}$ or $\mathscr{B}$. The number of aggressive agents is controlled by the parameter,

$$p_\alpha = N_A/N, \tag{2}$$

where $N_A = |\mathscr{A}|$ is the number of aggressive agents in a swarm, and p_α is constant in a swarm.

Analogous to the definition of the field of view, we define the field of aggression, $\mathcal{F}_{\alpha,i} = \mathcal{F}_\alpha(r_\alpha, \phi_\alpha; \boldsymbol{h}_i)$, for all agents $A_i \in \mathscr{A}$, which is a circular sector limited by the interaction length, $r_\alpha < r$, and the view angle, $\phi_\alpha < \phi$. While all agents have a field of view, the field of aggression is a property of only the aggressive agents.

The field of aggression $\mathcal{F}_{\alpha,i}$ is a sub-zone of $\mathcal{F}_{v,i}$, so the ratio $\tilde{\zeta}$ of their areas is

$$\tilde{\zeta} = r_\alpha^2 \phi_\alpha / r^2 \phi \leq 1 \ . \tag{3}$$

Agent A_i is triggered to behave aggressively when neighbors are present within $\mathcal{F}_{\alpha,i}$; these neighbors become potential targets of its aggressive behavior.

We associate an aggressive event with a temporary increase in the travel speeds of the agents involved in it. We call this temporary speed the burst speed, v_b, such that the speed ratio $\tilde{v}$ is

$$\tilde{v} = v_b/v_s > 1. \tag{4}$$

Both aggressive and non-aggressive agents can travel at burst speed.

Together, $p_\alpha, \tilde{v}, \tilde{\zeta}$, are the defining parameters of the new aggression model.

2.3 Aggressive behavior rules

In the aggression model, we define three new events to represent agonistic behavior: chase, bite-and-flight, and observe-and-avoid. These behaviors are anisotropic, as they result in selective attraction or repulsion of agents with their neighbors. The equations defining the kinematics of the chase, flight and avoidance are given in the Methods section (Section 5.2); here, we provide a sequential overview of them.

A chase is initiated by an aggressive agent, A_i, if any neighbors are located within its field of aggression $\mathcal{F}_{\alpha,i}$ (we term these as aggressive-zone neighbors). A chase results in the aggressive agent A_i bursting towards its nearest aggressive-zone neighbor. In essence, a chase is an attraction of an aggressor towards a target.

A bite occurs when a bursting aggressor comes within the distance τ (a tolerance) of a neighboring agent (the target agent). As a result of the bite, the attacker resumes steady behavior (travel at steady speed v_s), while the target initiates flight behavior, i.e., moves away from the attacker at burst speed v_b. A flight maneuver is the repulsion of an agent from its attacker.

An avoidance maneuver is performed by a non-aggressive agent, B_i, that observes a bursting aggressor. That is, if one or multiple aggressive agents enter the field of view of agent B_i at burst speed, then B_i bursts away from them. An avoidance maneuver is the repulsion of an agent from one or more potential attackers.

A schematic of pairwise interaction between an aggressive and non-aggressive agent is shown in Figure 2. In the top row, a chase, bite, and flight sequence is shown, while in the bottom row, an observe-and-avoid maneuver is shown. It should be noted that interactions among agents in a large swarm are much more complex than in Figure 2, and depend on $\tilde{v}$ and $\tilde{\zeta}$.

2.4 Quantifying aggression

Aggressive behavior results in discrete bursts and bites. To directly quantify the effect of aggression in a swarm, we introduce three new metrics: the rate of bites β, the rate of bursts σ, and the excess kinetic energy ratio E. To facilitate the definitions of these metrics, we define two averaging operators. The ensemble average over population $\mathscr{P}$ is denoted as, $\langle\cdot\rangle_{\mathscr{P}}$, and a time average is denoted as, $\overline{(\cdot)}^T$.

The rate of bites $\beta = \langle c_i/T_0\rangle_{\mathscr{P}}$ measures the average rate of bites received per agent in a swarm over the characteristic timescale T_0, where c_i is the number of bites received by agent $\mathcal{A}_i$, and $T_0 \equiv v_s/r\omega$ is defined based on the maximum turning rate ω. The timescale T_0 is representative of the timescale for cohesive collective behavior, and is equivalent to the timescale of one rotation of a mill [43].

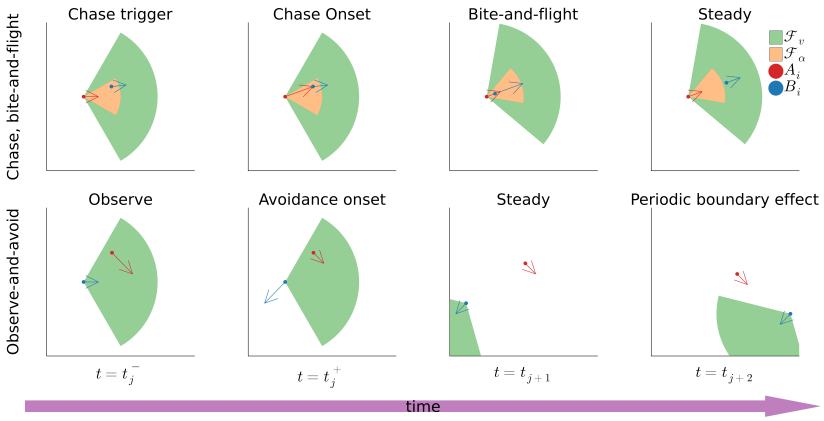


Fig. 2 Schematic of pairwise aggressive interactions. Top row: aggressor observes neighbor in field of aggression; aggressor initiates chase; aggressor bites target and resumes steady behavior, target initiates flight behavior; both agents are steady. Bottom row: non-aggressive agents observes bursting aggressive agent; non-aggressive agent initiates avoidance maneuver; avoidance successful, both agents are steady; periodic boundary effect.

Analogously, the rate of bursts $\sigma = \langle \delta t \ \overline{s_i(t)}^T \rangle_{\mathscr{S}}$ measures the average rate of bursts of agents in a swarm, based on the fraction of time spent bursting during a simulation. Here, s_i is a binary counter for bursts, where $s_i(t) = 0$ when $v_i(t) = v_s$ and $s_i(t) = 1$ when $v_i(t) = v_b$.

Finally, we define the excess kinetic energy ratio E of a swarm as the relative excess in kinetic energy of a swarm over an equivalent non-aggressive swarm where there is no bursting. Specifically, E is expressed as $E = V_0^2 - 1$, where $V_0 = \langle \overline{v_i(t)}^T / v_s \rangle_{\mathscr{S}}$ is the average normalized speed of the swarm during time interval T.

3 Results

We present here the results of extensive computational simulations of heterogeneous swarms where the proportion of aggressive agents in the swarm $p_\alpha \in [0, 1]$ is increased for a range of swarm densities ρ.

Introducing aggression to a swarm leads to a transition in steady-state collective behaviors driven by p_α. In Section 3.1, we first provide a qualitative overview of this transition, then we describe the transition mechanisms causing a shift in behavior, followed by a quantitative analysis of the steady-state phenomena present in the swarm. In Section 3.2, we discuss the welfare implications of aggression in a swarm.

3.1 Aggression-driven transition from milling to polarized order

In the absence of aggression, stable milling (rotation about a common center) is induced in swarms in the parameter range ($p_\alpha = 0$, $\rho \sim 5$, $v_s/r\omega \sim 1$, $\phi \sim \pi$) [43]. Here, we find that milling is unstable to aggression. That is, as the proportion of aggressive agents p_α increases, the steady-state collective behavior transitions from

milling to a polarized state (all headings are aligned). Within the polarized state, there is a smooth transition from unstructured flocking behavior (agents are randomly distributed) to structured banded behavior (agents are organized in parallel lines). This is summarized in Figure 3, where milling and banding behaviors are visually recognizable by agents forming ring shapes or parallel lines, while flocking agents are randomly distributed.

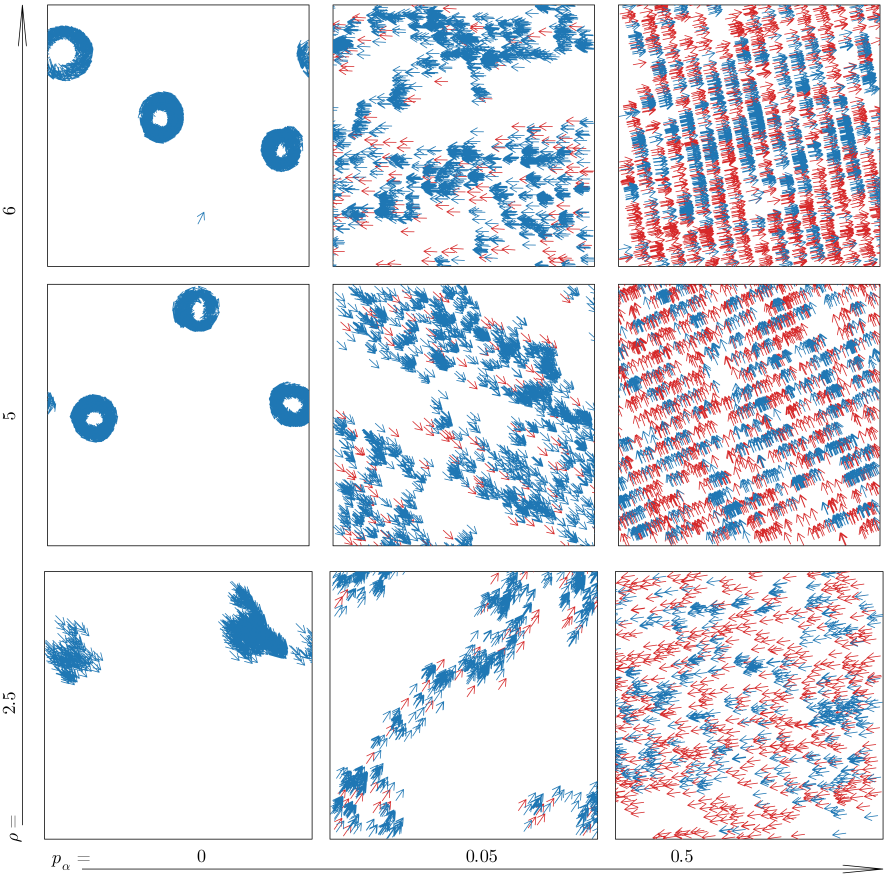


Fig. 3 Snapshots of swarm at steady state where each arrow represents the position and heading of an agent. Non-aggressive agents, are shown in blue, while aggressive agents are shown in red. In each snapshot, the swarm has a parameter pair (p_α, ρ), where the proportion of aggressors (p_α) increases along the horizontal axis, and the swarm density (ρ) increases along the vertical axis.

To facilitate the identification and quantitative analysis of the observed collective behaviors (e.g., the differentiation between milling, flocking, and banded behaviors), we develop a set of three global, swarm-level parameters: polarity P, milling duration T_M, and the banding parameter P_B. The polarity, or order parameter, $P(t)$ is a classical swarming metric measuring the degree of alignment of the swarm,

$P(t) = |\langle \boldsymbol{h}_i(t) \rangle_{\mathscr{S}}| \in [0, 1]$. We note that $P = \overline{P(t)}$, represents the time-averaged polarity during steady state. We define the mill duration, T_M, as the length of time during which a mill exists in a swarm. Mills are identified using the procedure outlined in Section 5.4. We also introduce a banding parameter, $P_B(t)$, defined as the harmonic energy density of the expression, $\mathcal{F}\{\boldsymbol{x} \cdot \hat{e}_{\parallel}\}$ (see Section 5.4), where $\mathcal{F}$ denotes the Fourier transform. The agent positions $(\boldsymbol{x} \cdot \hat{e}_{\parallel})$ are measured in the direction along the mean heading of the swarm. We define $P_B = \overline{P_B(t)}$ as the time-averaged banding parameter during steady state.

3.1.1 Transient phenomena

We start with a swarm where milling is stable ($v_s/r\omega = 1,\ \phi = \pi$) and $p_\alpha = 0$.

Even as small amounts of aggression are introduced ($p_\alpha \sim 0.01$), a time-dependent transition occurs where mills form then are destroyed by aggressive agents. Following mill destruction, the swarm transitions to a steady flocking state with high polarity ($P \sim 1$). An example of a mill destruction sequence is shown in the top row of Figure 4. Initially, a stable mill is formed (left frame). Then, aggressors cause milling agents to burst away from the mill, which breaks the mill (center frame). The mill destruction itself is a relatively short event, and its duration is typically on the order of the mill circular period. At a later time, the swarm has organized into flocking (third frame).

As p_α increases, the mill duration T_M decreases exponentially. By $p_\alpha \sim 0.1$, the mill duration is zero (i.e., milling is fully inhibited), and the steady-state polarity is near one ($P \sim 1$). That is, swarms in the range $p_\alpha \sim 0.1$ transition directly from disorder to flocking. An example sequence of this direct flocking formation is shown in the middle row of Figure 4.

To illustrate the effect of extremely low aggression ($p_\alpha \sim 10^{-4}$), we introduce a single aggressor into an otherwise homogeneous swarm where we would expect stable milling to occur. We find that with a single aggressor present, the collective behavior of the swarm is largely the same as in the homogeneous model, i.e., milling occurs and there is virtually no bursting ($\sigma \ll 1$). Specifically, we find a bi-stable state is possible where the swarm fragments into multiple groups, and some groups form stable mills while others are in a polarized flocking state. In the homogeneous swarm, it is typical for the swarm to fragment into multiple groups, and for all groups to form mills, though the same milling-flocking bi-stable state is possible [43]. A snapshot of a swarm with a single aggressor in a bi-stable state is shown in Figure 5, where in absence of noise or perturbation, the trajectory of the polarized fraction of the swarm will never intersect with the mills that have formed.

At intermediate values of aggression ($p_\alpha \sim 0.5$), another time-dependent transition takes place where a flocking swarm transitions to banded behavior. Banded agents are organized in parallel lines oriented orthogonally to the mean heading. The formation of bands is caused by aggressive herding. That is, in a single swarm, aggressors initiate an increasing number of chases and bites, which causes agents to, by sequential bursts, accumulate into a large herd (Figure 4, bottom left frame). Agents in the herd continue to burst (Figure 4, bottom center), instigated by chases and bites. Eventually, burst behavior causes the agents self-sort into evenly spaced bands (Figure 4, bottom right). The band spacing reduces the potential for agonistic behavior by placing agents outside

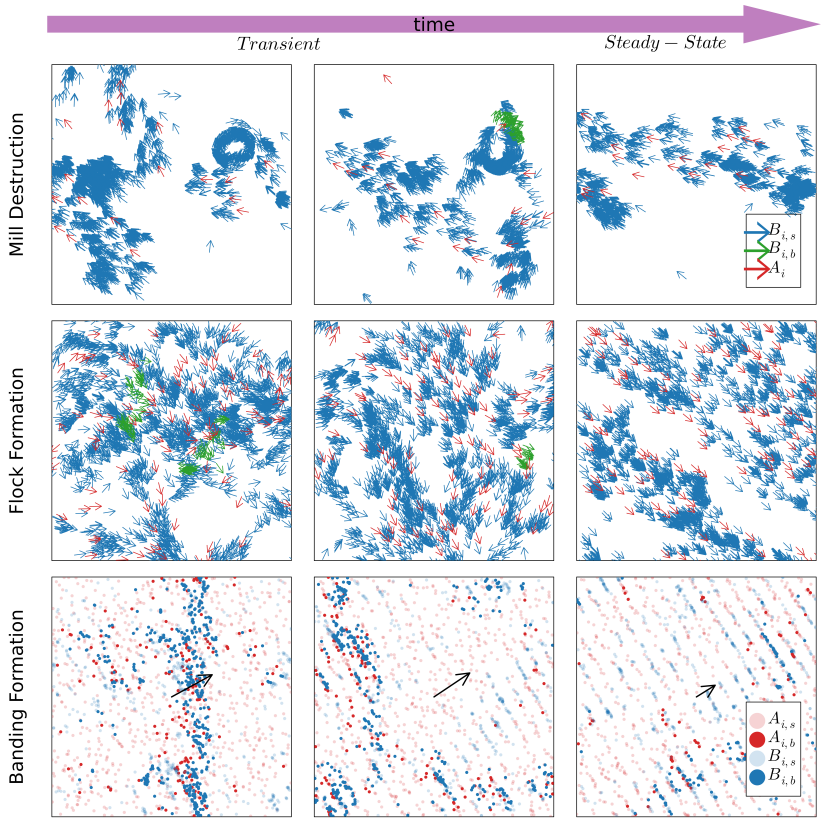


Fig. 4 Time evolution of collective behaviors to steady state. Top row: sample sequence of mill destruction. Mill is formed (*left*), the same mill is destroyed (*center*), after some time swarm is flocking (*right*). Middle row: Swarm gradually transitions over time from disorder to flocking. Bottom row: Herd forms inside flock (*left*). Agents continue to burst, organizing into bands and dissipating the herd (*center*). Agents are organized into parallel lines (bands) and are more steady (*right*). In the top two rows, agent positions and headings are represented by arrows where blue denotes a steady, non-aggressive agent, green denotes a bursting non-aggressive agent, and red denotes an aggressive agent. In the bottom row the swarm is highly polarized. Agent positions are shown with markers, and the mean velocity is shown with a single black arrow. Non-aggressive and aggressive agents are represented by blue and red markers, respectively. Steady and bursting agents are represented by transparent and opaque markers, respectively.

of the aggressive zones of their neighbors. The decrease in aggressive incidents is reflected in the reduced average speed of the swarm (less bursting).

While a banded swarm is generally moving at steady speed (shown by transparent markers in the bottom row of Figure 4), small groups of agents continue to burst sporadically (shown by opaque markers in the bottom row of Figure 4), then reorganize into bands. Even with intermittent bursting of agents, the banded behavior is stable. As such, banding behavior is quasi-steady; however, for simplicity it is referred to as a steady-state behavior.

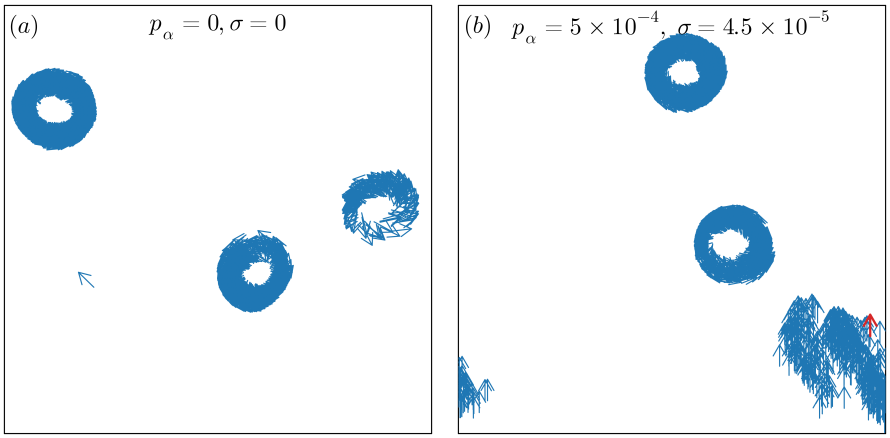


Fig. 5 Comparison of homogeneous non-aggressive swarm and a similar swarm when a single aggressor is introduced. (a) Homogeneous non-aggressive swarm during steady state, where virtually all agents are engaged in stable milling behavior. (b) Swarm with single aggressor (red arrow) in bi-stable state, where part of the swarm is milling and part of the swarm is flocking. The rate of bursts (σ) is nearly zero, similarly to the homogeneous swarm. All agent positions and headings are represented by an arrow.

3.1.2 Steady-state phenomena

In Figure 3, snapshots of the swarm show the transition of steady-state collective behavior from milling to flocking to banding as the proportion of aggressors increases ($p_\alpha = [0, 0.05, 0.5]$). Additionally, Figure 3 shows that both milling and polarized behavior are dependent on the swarm density, ρ. We note that the behavior at $\rho = 5, 6$ is largely the same, while the behavior at $\rho = 2.5$ differs; this illustrates the nonlinear relationship of collective behavior to swarm density, ρ. Here, we focus on quantifying the steady-state collective phenomena, and their relationship to p_α and ρ.

At $p_\alpha > 0$, there is virtually no steady-state milling in the swarm. Rather, the steady-state behavior of the swarm is polarized (all headings are aligned; $P \gtrsim 0.8$).

As p_α increases, a transition occurs in the polarized phase between flocking, where agents are randomly distributed in space, and banding, where agents are organized into parallel lines. The banding parameter, $P_B \in [0, 1]$, measures how strongly agents are organized into parallel lines. When agents' positions are unstructured (flocking), the banding parameter is low ($P_B \sim 0.3$), and when they are structured (parallel lines), the banding parameter is high ($P_B \sim 0.9$). In the intermediate range, $0.3 \lesssim P_B \lesssim 0.9$, some parts of the swarm may be banded while others are unstructured.

The aggression-driven transition between the steady-state behaviors is summarized in Figure 6a by the polarity P and the banding parameter P_B. For low-aggressive swarms ($p_\alpha \lesssim 0.1$), flocking is the predominant behavior ($P_B \lesssim 0.3$). In the range of $0.1 \lesssim p_\alpha \lesssim 0.4$, P_B increases nearly linearly; here, the swarm gradually (with respect to p_α) organizes its positions from randomly distributed to parallel lines. In the intermediate-aggressive range, $0.4 \lesssim p_\alpha \lesssim 0.8$, swarms are strongly banded, and

the banding parameter is relatively constant ($P_B \sim 0.9$). At high aggressive proportions ($p_\alpha \gtrsim 0.8$), swarms become more homogeneously aggressive, and banding behavior declines. This indicates that a binary population is necessary for banding to occur — when the swarm is over-saturated with aggressors, unstructured flocking is reestablished.

The spectrum of behavior between flocking and banding varies with swarm density, ρ, as well as with p_α (see Figures 6*b*, 3). Strong banding occurs at higher swarm densities ($\rho \sim [4, 6]$), while flocking dominates at low densities ($\rho \sim 2.5$).

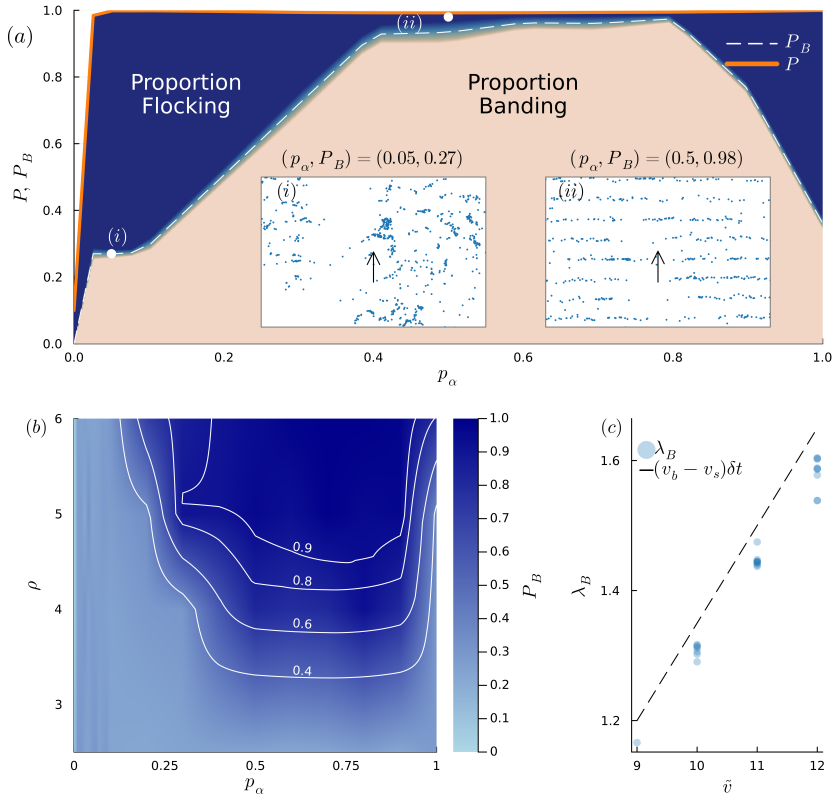


Fig. 6 Characteristics of steady-state collective behaviors. (*a*) The transition between flocking and banding behaviors as a function of the proportion of aggressors (p_α). The average steady state polarity of a swarm (P) is shown by an orange line, where the thickness of the line represents the 95% confidence band; the average banding parameter (P_B) is shown by white dashed line. The shaded section (light tan) below P_B represents the proportion of swarms that are banded, and the shaded section (dark blue) between P_B and P represents the proportion of swarms that are flocking. The color gradient between the tan and blue shaded sections is the 95% confidence band of P_B. The inset plots (i), (ii) show examples of flocking and banded swarms, respectively, corresponding to the displayed values of (p_α, P_B); agent positions are shown with blue markers and mean swarm velocity is shown with a black arrow. (*b*) Banding parameter (P_B, blue gradient) varies with p_α and swarm density ρ; contour lines are in white. (*c*) Banding separation (λ_B, blue markers) is correlated with speed ratio $\tilde{v}$ and approximated by $\delta x = (v_b - v_s)\delta t$ (black dotted line).

Banding behavior is characterized by agents organized into parallel lines of relatively equal spacing. The banding separation or wavelength, λ_B, correlates with the spatial difference $\delta x = (v_b - v_s)\delta t$ (see Figure 6*c*). This relationship can be qualitatively explained in terms of bite-and-flight behavior. In Figure 2, we note that a bite causes an aggressor to resume steady speed v_s, while the target engages in flight behavior and advances at burst speed, v_b. If the headings of the aggressor and target are aligned, then their separation at the next decision time is on the order of δx. In section 3.1.1, we show that banding results from repetitive bites, causing the swarm to self-organize into parallel lines. The spacing, δx, results in agents in one row to generally be outside of the aggressive range of agents in neighboring rows. As agents get bitten then separate by the distance δx, parallel lines gradually form, aggressive potential reduces, and the swarm enters steady banded behavior.

Among the model parameters governing individual behavior, the burst speed ratio $\tilde{v}$ has the most significant consequences on the dynamics of the swarm. These swarm-level dynamics are affected by $\tilde{v}$-dependent spatial relationships between agents. While δx $(= \delta t v_s(\tilde{v} - 1))$ determines the banding separation, the ratio $v_b \delta t/r$ $(= \tilde{v} v_s \delta t/r)$ relates to how accurately an attacker will approach a target, and to how successfully an agent will escape an attacker. Motivated by burst-to-steady speed ratios in animals (see Section 2.1), all simulations in Section 3 (with the exception of the simulations for Figure 6c) are performed with $\tilde{v} = 10$. We note that at $\tilde{v} = 10$, the rate of bursts σ has attained its asymptotic value, Section 5.3.

This $\tilde{v}$-dependent individual behavior strongly affects the collective behavior — an order of magnitude decrease in $\tilde{v}$ changes the steady behavior from flocking to fronts (see Figure 8*b*-*e*). By contrast, the collective behavior is less sensitive to the zone-area ratio $\tilde{\zeta}$; an order of magnitude difference in $\tilde{\zeta}$ causes relatively little change to the swarm characteristics (Figure 8*b*-*e*). Hence, without loss of generality, $\tilde{\zeta} = 1/16$ is used for all simulations in Section 3. The variation of the rate of bursts σ in a swarm for different $\tilde{v}$ and $\tilde{\zeta}$ is described in detail in Section 5.3.

3.2 Welfare implications

The presence of aggression in a swarm can have profound effects on its welfare. Here, we consider the welfare characteristics of our simulated swarms using two metrics, related to (i) energetics and (ii) the number of bites observed per agent.

Aggressive behavior causes an increase in the energy consumption of the swarm, as agents spend more energy to burst. A direct way to measure the energy of the swarm is by the excess kinetic energy ratio, E.

In steady-state collective behaviors, such as banding, aggressors drive an ordered, low-energy phase. We measure E for aggressive and non-aggressive agents, averaged during the transient phase and during steady-state (Figure 7*a*). For all agents, the kinetic energy drops by an order of magnitude from the transient phase to the steady-state phase, even as aggression is present. This shows that while aggression tends to increase the energy consumption in the swarm, the steady-state ordered phases of the aggressive swarm are in fact energetically inexpensive, relative to the disordered transition phase.

The increase in energy expenditure due to aggression disproportionally affects non-aggressive agents. Whether in the transient phase or steady-state, the average excess energy of non-aggressive agents ($E_{B,\mathrm{tr}}$, $E_{B,\mathrm{ss}}$, respectively) tends to be higher (by up to 80% at high densities) than that of aggressive agents ($E_{A,\mathrm{tr}}$, $E_{A,\mathrm{ss}}$):

$$E_{B,\mathrm{tr}} > E_{A,\mathrm{tr}} \quad , \quad E_{B,\mathrm{ss}} > E_{A,\mathrm{ss}} \; . \tag{5}$$

This results from the asymmetric nature of our aggression rules: we assume that aggressors cannot burst to attack consecutively, while non-aggressive agents can burst to escape infinitely (Section 5.2). This causes disparate energy spending for aggressive and non-aggressive agents.

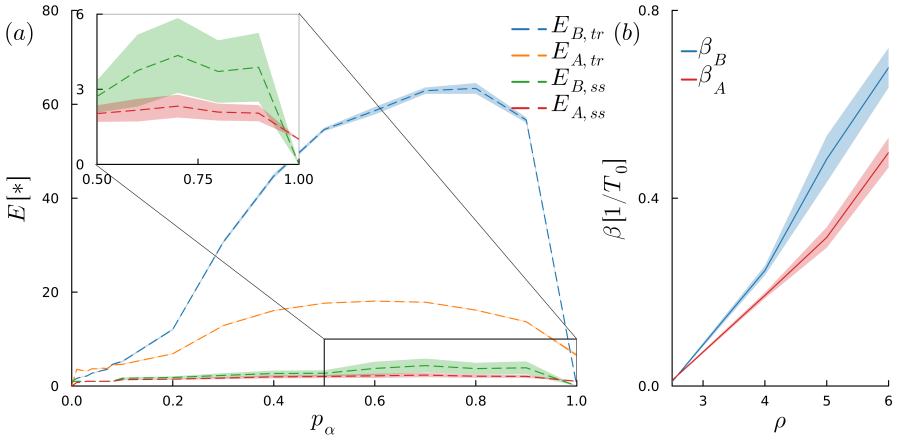


Fig. 7 Welfare characteristics in aggression-driven swarms. (a) Kinetic energy ratio E varies with p_α, and is larger during the transient period (E_{tr}) than during steady state (E_{ss}). Energy is larger for non-aggressive agents (E_B) than for aggressive agents (E_A). (b) The average rate of bites β per agent in a swarm (shown for $p_\alpha = 0.5$) is correlated with the swarm density ρ. The rate of bites is generally higher for non-aggressive agents (β_B) than for aggressive agents (β_A). The 95% confidence bands are shown as shaded areas in both plots.

To measure the direct effect of aggressive attacks on agents in our simulations, we track the number of bites β received per agent in a swarm. As the proportion of aggressors p_α increases, the rate of bites β increases then decreases similarly to the kinetic energy ratio E in Figure 7*a*. By contrast, β is directly correlated with the swarm density, ρ (Figure 7*b*). That is, even for a highly mixed population (e.g., $p_\alpha = 0.5$), β is near zero at low swarm density, while it approaches one at higher densities. This indicates that swarm density plays a critical role in controlling agonistic behavior in a swarm. Interestingly, for high densities and intermediate p_α, the rate of bites is higher for non-aggressive agents (β_B) than it is for aggressive agents (β_A).

Together, the kinetic energy ratio, E, and the rate of bites, β, compose a welfare indicator for a swarm. The addition of aggression to a swarm causes agents to spend more energy and to be bitten more often. This may lead to exhaustion from excessive

energy spending, and to poor health since bites increase the risk of disease. The deterioration of agent welfare is exacerbated by swarm density. Additionally, non-aggressive agents spend more energy and receive more bites, which increases the disparity of the swarm.

We note that both the energy spent E and the rate of bites β are non-monotonically related to the proportion of aggressors, p_α. This is a consequence of the asymmetry of the behavioral rules; i.e., aggressive agents to not attack continuously, but non-aggressive agents can perform avoidance maneuvers infinitely (see Methods, Section 5.2).

4 Discussion

We present a novel model for aggression in swarms, built on heterogeneous animal-like behavioral rules. These govern the behavior and interaction of aggressive and non-aggressive self-propelled agents. To our knowledge, this is the first model to simulate animal-like aggression in this way. The model indicates the existence of new ordered collective states and offers a detailed look into the agent- and swarm-level effects of aggression.

We introduce new heterogeneous behavioral rules based on anisotropic selective attraction and repulsion, combined with unsteady kinematics. These newly defined behaviors simulate chases, bites, and escape maneuvers, similar to agonistic behavior in animal groups. These aggression-induced behaviors result in speed variability of the agents, i.e., agents involved in aggressive events temporarily increase their speed (burst). The model also provides a baseline of quantitative measure for the relative increase of bursts and bites within the swarm, based on the fraction of aggressors p_α in the population, and the density ρ of the swarm.

Using simulations with $\mathrm{O}(10^3)$ agents, we find that mills, rotating collective states that are stable in homogeneous swarms, are highly unstable to aggression. That is, even a small proportion of aggressive agents ($p_\alpha \sim 0.01$) in the swarm can destroy stable mills.

However, aggression does not always act as a destructive force; rather, it drives the swarm to new ordered states. With enough aggressors present ($p_\alpha \sim 0.1$), milling is fully inhibited and the swarm transitions directly from disorder to polarized flocking. At intermediate levels of aggression ($p_\alpha \sim 0.5$), herding instigated by bites and chases from aggressors transitions the swarm from flocking to banding — a collective state with a higher degree of order than flocking (agents are aligned in parallel lines).

The steady ordered states resulting from aggressive behavior are energetically inexpensive relative to the transient disordered states. As an aggressive heterogeneous swarm organizes from disorder to order, the energy spending of the swarm decreases by an order of magnitude. The steady-state energetic cost of an aggressive heterogeneous swarm is on the same order as an equivalent homogeneous non-aggressive swarm. In short, highly ordered states like flocking or banding require little energy to maintain, relative to the excess energy needed to establish the order. The energy increase E is not evenly distributed between aggressive and non-aggressive agents. Non-aggressive agents spend more energy per agent on average than aggressive agents.

Our results show that the rate of bites β is directly correlated with swarm density. At high densities ($\rho \in [4, 6]$), β exhibits a similar trend to energy E as a function of p_α — increasing for $p_\alpha \lesssim 0.8$ and decreasing for larger p_α. These results indicate that density plays a crucial role in the welfare of the swarm.

The new model for animal-like aggression in swarms and the results presented here are of both theoretical and practical interest. With respect to theoretical interest, the model and the results offer insight into the new aggression-driven transition of collective behavior in a heterogeneous swarm. The results are also of practical importance as they assess the energetic cost of aggression and wear from bites on a swarm. Our findings on swarm energy spending and welfare could be useful to industries relying on animal groups — a relevant example is fin-fish aquaculture.

In a fish farm, the energy spending of the swarm determines feed requirement, at great economic consequence. Relative to a non-aggressive baseline, we show that aggression causes an increase in the kinetic energy of a swarm by almost 6 times during steady state, and up to 60 times in the transient regime. While true cost of transport relies on several factors additional to kinetic energy [44–46], our results show that aggression has a significant impact on swarm energy consumption and should be taken into account. When applied to fish in this way, our model may help to inform the welfare conditions of fin-fish aquaculture farms. Aggression in fish is known to cause chronic stress, and bite-related fin damage and infection, affecting both the welfare of the fish and the success of the farm. Additionally, disease in fish farms is often treated with excessive antimicrobial use [26], which can pose health risks to the consumer [27]. Furthermore, severe burst exercise in fish can cause exhaustion and sometimes death [47, 48]. With our model, we can quantify both burst exercise and the rate of bites per fish.

The model developed here is the first heterogeneous swarming model for animal-like aggression. As such, it includes a number of simplification that could be improved in future models. In terms of social interactions, aggressive and neighbor-neighbor interaction rules could be modified. For example, rather than specifying a fixed proportion of agents that are aggressive, a probability of aggression could be assigned to each agent. Specific neighbor-neighbor rules could be adjusted, such as introducing a probabilistic direction of escape in avoidance and flight maneuvers to account for errors in judgment. In addition, other behavioral rules, such as homogeneous attraction and repulsion, could be added. For a more physical approach, a dynamical model of each agent could be introduced to constrain agent response to realistic, smooth accelerations. To further improve the feasibility of behavior, an energy reservoir ("battery") could be introduced to each agent, where bursting would result in energy depletion. An energy budget could suppress bursting when energy is overly depleted, such that bursting cannot be performed infinitely (akin to sustained and burst swimming in fish, powered by red and white muscles, respectively [49, 50]). Finally, for a physically accurate model of fish schooling, an extension of the current model from two to three dimensions and modeling of hydrodynamic interactions between fish would be necessary.

Overall, our results are suggestive of collective behaviors seen in nature, such as aggression among fish, sheep herded by dogs, and marching bands of locusts. We show

that behavioral heterogeneity and unsteadiness have significant consequences on the collective behavior and energy spending of the swarm by clear visual and quantitative metrics. Our results on the collective behavior, energy spending, and welfare of an aggressive heterogeneous swarm may apply broadly to understanding animal behavior.

5 Methods and additional results

5.1 Homogeneous Model

The homogeneous model replicates the Vicsek-based minimal milling model [33]. The agents, $\mathcal{A}_i$, with state, $\mathcal{S}_i(t) = \mathcal{S}(\boldsymbol{x}_i(t), \boldsymbol{h}_i(t); v_i(t))$, are initiated with randomly distributed positions ($\boldsymbol{x}_i(t)$) and headings ($\boldsymbol{h}_i(t)$), and with steady speed ($v_i(t) = v_s$). Each agent $\mathcal{A}_i$ has a neighborhood $\mathcal{N}_v^i = \{\mathcal{A}_k \in \mathscr{S} : \boldsymbol{x}_k \in \mathcal{F}_{v,i}\}$, composed of the $|\mathcal{N}_v^i|$ neighbors within its field of view, $\mathcal{F}_{v,i} = \mathcal{F}_v(r, \phi; \boldsymbol{h}_i(t))$ (schematic of field of view shown in Figure 2). At each decision time t_j, each agent acts to align its heading with that of its neighbors,

$$\tilde{\boldsymbol{h}}_i'(t_{j+1}) = \langle \boldsymbol{h}_k(t_j) \rangle_{\mathcal{N}_v^i} \tag{6a}$$

$$\tilde{\boldsymbol{h}}_i(t_{j+1}) = \text{norm}\left(\tilde{\boldsymbol{h}}_i'(t_{j+1})\right) . \tag{6b}$$

Here, $\text{norm}\,(\boldsymbol{v}) = \boldsymbol{v}/||\boldsymbol{v}||$ represents normalization of vector $\boldsymbol{v}$.

The desired heading, $\tilde{\boldsymbol{h}}_i(t_{j+1}) = [\cos(\tilde{\theta}_i(t_{j+1})),\ \sin(\tilde{\theta}_i(t_{j+1}))]$, is constrained by the maximal turning rate ω, such that the attained angular heading is defined as,

$$\theta_i(t_{j+1}) = \begin{cases} \theta_i(t_j) + \delta\theta_i + \Delta\theta_i & ,\ |\delta\theta_i| < \omega\delta t \\ \theta_i(t_j) \pm \omega\delta t + \Delta\theta_i & ,\ |\delta\theta_i| \geq \omega\delta t, \end{cases} \tag{7}$$

where the sign preserves the direction of rotation that would take place without any limit to the turning rate, and the desired turning angle $\delta\theta_i$ is defined as, $\delta\theta_i = \tilde{\theta}_i(t_{j+1}) - \theta_i(t_j)$. The time increment, δt, represents the reaction time of an agent. The angle $\Delta\theta_i$ acts as a random fluctuation in heading, and is uniformly distributed as $\Delta\theta_i \in \mathcal{U}(-\eta/2, \eta/2)$. In all of our simulation, noise is not present ($\eta = 0$).

5.2 Aggression Model

We define three neighborhoods (sets of neighboring agents) associated with spatial parts of the domain. The neighborhood $\mathcal{N}_v^i$ associated with the field of view $\mathcal{F}_{v,i}$ is defined for every agent $\mathcal{A}_i$ in the swarm $\mathscr{S}$. The aggressive-zone neighborhood $\mathcal{N}_\alpha^i = \{\mathcal{A}_z \in \mathscr{S} : \boldsymbol{x}_z \in \mathcal{F}_{\alpha,i}\}$ is the set of all neighbors located within the field of aggression $\mathcal{F}_{\alpha,i} = \mathcal{F}_\alpha(r_\alpha, \phi_\alpha; \boldsymbol{h}_i)$, defined for aggressive agents ($A_i \in \mathscr{A}$) only. Finally, the subset of aggressive-zone neighbors that are within a distance τ of agent A_i, $|\boldsymbol{x}_z - \boldsymbol{x}_i| < \tau$, compose the set, $\mathcal{N}_\tau^i$. These are the neighbors close enough to A_i to be bitten, where $\tau < r_\alpha$ acts as a tolerance distance.

We introduce three new behaviors resulting from neighbor-neighbor interactions: chase, bite-and-flight, and observe-and-avoid, which are described subsequently, along

with their respective onset and offset conditions. All agents not engaged in a chase, flight, or avoidance maneuver resume or continue steady behavior.

5.2.1 Chase

A chase is qualified as a short attack that can be initiated at t_{j+1} by an aggressive agent A_i that is traveling at a steady speed ($v_i(t_j) = v_s$) and is not engaged in bite behavior at t_j. If there are agents in its aggressive-zone neighborhood ($|\mathcal{N}_\alpha^i| > 0$), agent A_i starts pursuing its nearest aggressive-zone neighbor, $\mathcal{A}_z$, with burst speed v_b. As a result, the velocity update for agent A_i is such that,

$$v_i(t_{j+1}) = v_b \tag{8a}$$

$$\tilde{\boldsymbol{h}}_i(t_{j+1}) = \text{norm}\left(\boldsymbol{x}_z(t_j) - \boldsymbol{x}_i(t_j)\right). \tag{8b}$$

As the goal of a chase is not to capture, but to display aggression, the chase behavior is automatically offset after one decision time. This prevents an infinite chase-escape pairwise loop.

5.2.2 Bite-and-flight

A bite is an instantaneous pairwise aggressive event, and exists when an aggressive chasing agent A_i comes into close proximity (i.e., within τ) to any agent within its field of aggression, $\mathcal{F}_{\alpha,i}$. That is, a bite at time t_j may be caused by an agent A_i that has been engaged in a chase ($v_i(t_j) = v_b$). If A_i has $|\mathcal{N}_\tau^i| > 0$ aggressive-zone neighbors within the tolerance distance τ, then agent A_i bites a random agent $\mathcal{A}_l$ from $\mathcal{N}_i^\tau$.

As a result of the bite, agent A_i (the biter) resumes steady behavior as defined in Section 5.1, while neighbor $\mathcal{A}_l$ (the target) begins flight behavior, i.e., bursts away from the biter. That is, at time t_j the velocity update for agent $\mathcal{A}_l$ is given by,

$$v_l(t_{j+1}) = v_b \tag{9a}$$

$$\tilde{\boldsymbol{h}}_i(t_{j+1}) = \text{norm}\left(\boldsymbol{x}_l(t_j) - \boldsymbol{x}_i(t_j)\right). \tag{9b}$$

Only an aggressive agent can initiate a bite; however, any agent that has been bitten engages in the flight behavior described by equation (9), whether aggressive or non-aggressive.

5.2.3 Observe-and-avoid

An avoidance maneuver at t_{j+1} occurs when a non-aggressive agent B_i that was not bitten at t_j observes a bursting aggressive agent in its field of view, $\mathcal{F}_{v,i}$. That is, if an agent B_i has a non-empty set of neighbors $\mathcal{N}_{\text{a}}^i \subseteq \mathcal{N}_v^i$, where $\mathcal{N}_{\text{a}}^i = \{A_w \in \mathcal{N}_v^i : v_w = v_b,\ A_w \in \mathscr{A}\}$, then agent B_i performs an avoidance maneuver, i.e., moves away from the aggressors in $\mathcal{N}_{\text{a}}^i$. The velocity update for agent B_i is given by

$$v_i(t_{j+1}) = v_b \tag{10a}$$

$$\tilde{\boldsymbol{h}}_i(t_{j+1}) = \text{norm}\left(\langle \boldsymbol{x}_i(t_j) - \boldsymbol{x}_w(t_j)\rangle_{\mathcal{N}_{\text{a}}^i}\right). \tag{10b}$$

5.3 Sensitivity of collective behavior to aggressive model parameters

The effects of the aggressive behaviors described in Section 5.2 on the collective response of the swarm depend on the burst speed ratio $\tilde{v}$ and the zone-are ratio $\tilde{\zeta}$. As expected, the characteristics of collective behavior change when the values of $\tilde{v}$ and $\tilde{\zeta}$ are in different ranges, Figure 8.

Quantitatively, Figure 8*a* shows how the rate of bursting, σ, varies with $\tilde{v}$ and $\tilde{\zeta}$ at $p_\alpha = 0.1$. An asymptotic value for σ is achieved for $\tilde{v} \gtrsim 8$ (when $\tilde{\zeta} = 1/16$), and for $\tilde{\zeta} \gtrsim 1/2$ (when $\tilde{v} = 8$). (We note that the rate of bites β behaves nearly identically to σ with respect to $\tilde{v}$ and $\tilde{\zeta}$, and is not included here.) Qualitatively, Figures 8*b*-*e* show snapshots of steady state behavior varying with with $\tilde{v} = \{2, 10\}$ and $\tilde{\zeta} = \{1/16, 1/2\}$ for $p_\alpha = 0.1$; similarities are shared between swarms with differing $\tilde{\zeta}$ but with the same $\tilde{v}$. That is, for both $\tilde{\zeta} = \{1/16, 1/2\}$, fronts form with $\tilde{v} = 2$ while polarized flocking takes place when $\tilde{v} = 10$.

Noting the rate of bursts σ for each snapshot in Figure 8*b*-*e*, we find that increasing $\tilde{\zeta}$ and decreasing $\tilde{v}$ both have the effect of increasing the rate of bursts. This can be explained by the increase in the zone-area ratio $\tilde{\zeta}$ expanding the potential for aggressive stimulus. Conversely, decreasing the speed ratio, $\tilde{v}$, reduces an agent's ability to escape.

5.4 Identifying steady collective states

5.4.1 Mill identification method

Mills are identified in all simulations (irrespective of p_α) with the following method. At a given time t_j, agents are first grouped by the sign of their rotation over the previous decision time, t_{j-1}. A clustering algorithm is then used to group agents based on proximity. A mill is identified in clusters where the polarity $P \lesssim 0.5$, the cluster angular momentum about its own center A_M is such that $\frac{\omega}{v_s^2}\overline{A_M} \gtrsim 0.5$, and the cluster center is relatively stationary. All time-averaged quantities are averaged over two circular periods $T_0 = v_s/r\omega$.

5.4.2 Banding parameter

The banding parameter $P_B(t) \in [0, 1]$ measures how strongly agents in a polarized swarm are distributed in parallel lines. At a given time the agent positions along the mean heading of the swarm are $\boldsymbol{x} \cdot \hat{e}_\parallel$. If the swarm is banded, then the discrete Fourier transform $F(k_j) = \mathcal{F}\{\boldsymbol{x} \cdot \hat{e}_\parallel\}$ will have a distinct peaks at the banding wavenumber and its harmonic wavenumbers (the harmonics come from the differences in agent densities within each band).

As banding is related to neighbor-neighbor interactions on the order of the interaction length r, we identify the tallest peak of $F(k_j)$ near $k = 2\pi/r$ ($F(k_i^*)$, $i = 0$) and its harmonics ($i = 1, 2, ...$). We apply an amplitude filter, where if $F(k_j) < F(k_0^*)/3$ then $F(k_j) = 0$. Finally, using the filtered signal, the banding parameter is defined as, $P_B = \sum F(k_i^*) / \sum F(k_j)$.

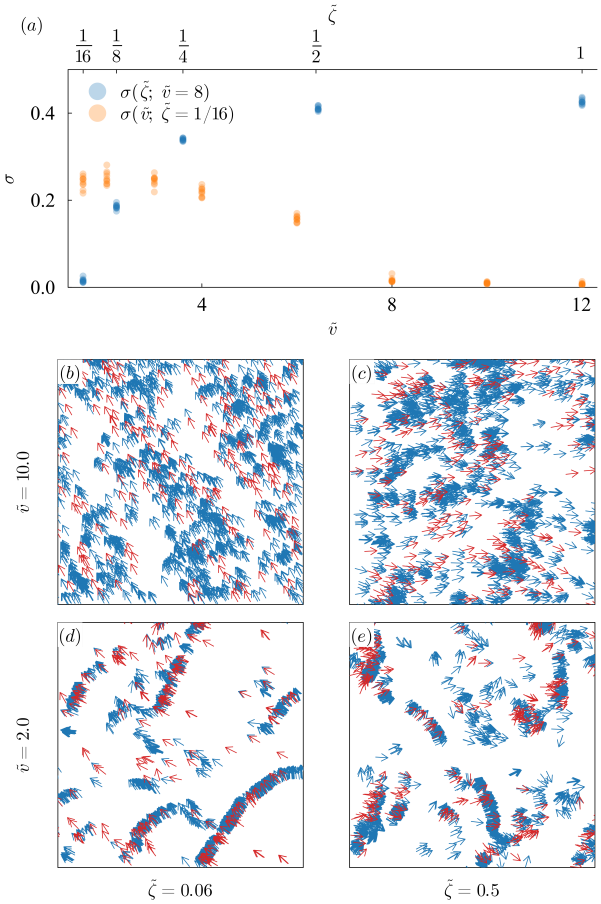


Fig. 8 Effect of varying $\tilde{v}$ and $\tilde{\zeta}$ in an aggressive swarm. (a) The dependence of the rate of bursts σ on the speed ratio $\tilde{v}$ (orange markers) and on the zone-area ratio $\tilde{\zeta}$ (blue markers). (b)-(e) Snapshots of swarm at steady state with varying $(\tilde{\zeta}, \tilde{v})$, where the measured rate of bursts $\sigma =$ (b): 0.01, (c): 0.4, (d): 0.3, (e): 0.4. Aggressive agents are shown in red and non-aggressive agents are shown in blue. All plots in this figure have $p_\alpha = 0.1$.

Declarations

Funding

This research is supported financially by grants from MIT Sea Grant No. 2024-R/RRFA-022.

This material is based upon work supported by the National Science Foundation Graduate Research Fellowship Program (for F.G.) under Grant No. 2141064. Any opinions, findings, and conclusions or recommendations expressed in this material are those of the authors and do not necessarily reflect the views of the National Science Foundation.

Competing Interests

The authors have no competing interests to declare.

Ethics approval and consent to participate

Not applicable.

Consent for publication

Not applicable.

Data and materials availability

The datasets used and/or analyzed during the current study are available from the corresponding author on reasonable request.

Code availability

The code used in this study is available upon request from the corresponding author.

Author Contributions

Conceptualization: F.G, G.T, D.K.P.Y; **Data curation:** F.G.; **Formal analysis:** F.G.; **Funding acquisition:** F.G., D.K.P.Y.; **Investigation:** F.G.; **Methodology:** F.G., G.T., D.K.P.Y.; **Project administration:** D.K.P.Y.; **Software:** F.G.; **Supervision:** G.T., D.K.P.Y.; **Validation:** F.G.; **Visualization:** F.G.; **Writing - original draft:** F.G.; **Writing - review and editing:** F.G., G.T., D.K.P.Y.

References

[1] Vicsek, T. & Zafeiris, A. Collective motion. Physics Reports **517**, 71–140 (2012). URL https://linkinghub.elsevier.com/retrieve/pii/S0370157312000968.

[2] De, R. & Chakraborty, D. Collective motion: Influence of local behavioural interactions among individuals. Journal of Biosciences **47**, 48 (2022). URL https://link.springer.com/10.1007/s12038-022-00277-4.

[3] Ioannou, C. C. & Laskowski, K. L. A multi-scale review of the dynamics of collective behaviour: from rapid responses to ontogeny and evolution. Philosophical Transactions of the Royal Society B **378**, 20220059 (2023). URL https://royalsocietypublishing.org/rstb/article/378/1874/20220059/109127/A-multi-scale-review-of-the-dynamics-of-collective.

[4] Gu, F., Guiselin, B., Bain, N., Zuriguel, I. & Bartolo, D. Emergence of collective oscillations in massive human crowds. Nature **638**, 112–119 (2025). URL https://www.nature.com/articles/s41586-024-08514-6.

[5] Hemelrijk, C. K. & Hildenbrandt, H. Schools of fish and flocks of birds: their shape and internal structure by self-organization. Interface focus **2**, 726 (2012).

[6] Tunstrøm, K. et al. Collective States, Multistability and Transitional Behavior in Schooling Fish. PLoS Computational Biology **9**, e1002915 (2013). URL https://dx.plos.org/10.1371/journal.pcbi.1002915.

[7] Trucco, A. Applying collective motion models to study discordant individual behaviours within a school of fish. Royal Society Open Science **10**, 231618 (2023). URL https://royalsocietypublishing.org/doi/10.1098/rsos.231618.

[8] Pourpanah, F., Wang, R., Lim, C. P., Wang, X.-Z. & Yazdani, D. A review of artificial fish swarm algorithms: recent advances and applications. Artificial Intelligence Review **56**, 1867–1903 (2023). URL https://link.springer.com/10.1007/s10462-022-10214-4.

[9] Calovi, D. S. et al. Swarming, schooling, milling: phase diagram of a data-driven fish school model. New Journal of Physics **16**, 015026 (2014). URL https://iopscience.iop.org/article/10.1088/1367-2630/16/1/015026.

[10] Zampetaki, A., Yang, Y., Löwen, H. & Royall, C. P. Dynamical order and many-body correlations in zebrafish show that three is a crowd. Nature Communications **15**, 2591 (2024). URL https://www.nature.com/articles/s41467-024-46426-1.

[11] Papaspyros, V. et al. Predicting the long-term collective behaviour of fish pairs with deep learning. Journal of The Royal Society Interface **21**, 20230630 (2024). URL https://royalsocietypublishing.org/doi/10.1098/rsif.2023.0630.

[12] Ko, H., Lauder, G. & Nagpal, R. The role of hydrodynamics in collective motions of fish schools and bioinspired underwater robots. Journal of The Royal Society Interface **20**, 20230357 (2023). URL https://royalsocietypublishing.org/doi/10.1098/rsif.2023.0357.

[13] Pan, Y. & Lauder, G. V. Combining Computational Fluid Dynamics and Experimental Data to Understand Fish Schooling Behavior. Integrative And Comparative Biology **64**, 753–768 (2024). URL https://academic.oup.com/icb/article/64/3/753/7676182.

[14] Jolles, J. W., King, A. J. & Killen, S. S. The role of individual heterogeneity in collective animal behaviour. Trends in ecology & evolution **35**, 278–291 (2020).

[15] Muro, C., Escobedo, R., Spector, L. & Coppinger, R. Wolf-pack (Canis lupus) hunting strategies emerge from simple rules in computational simulations. Behavioural Processes **88**, 192–197 (2011). URL https://linkinghub.elsevier.com/retrieve/pii/S0376635711001884.

[16] Strömbom, D. et al. Solving the shepherding problem: heuristics for herding autonomous, interacting agents. Journal of The Royal Society Interface **11**, 20140719 (2014). URL https://royalsocietypublishing.org/doi/10.1098/rsif.2014.0719.

[17] Gómez-Nava, L., Bon, R. & Peruani, F. Intermittent collective motion in sheep results from alternating the role of leader and follower. Nature Physics **18**, 1494–1501 (2022). URL https://www.nature.com/articles/s41567-022-01769-8.

[18] Weinburd, J. et al. Anisotropic interaction and motion states of locusts in a hopper band. Proceedings of the Royal Society B: Biological Sciences **291**, 20232121 (2024). URL https://royalsocietypublishing.org/doi/10.1098/rspb.2023.2121.

[19] Guttal, V., Romanczuk, P., Simpson, S. J., Sword, G. A. & Couzin, I. D. Cannibalism can drive the evolution of behavioural phase polyphenism in locusts. Ecology Letters **15**, 1158–1166 (2012). URL https://onlinelibrary.wiley.com/doi/10.1111/j.1461-0248.2012.01840.x.

[20] Couzin, I. D. & Couzin-Fuchs, E. The chemical ecology of locust cannibalism. Science **380**, 454–455 (2023). URL https://www.science.org/doi/10.1126/science.adh5264.

[21] Damsgård, B. & Huntingford, F. in *Fighting and Aggression* (eds Huntingford, F. A., Jobling, M. & Kadri, S.) Aquaculture and Behavior 248–285 (Wiley-Blackwell, Chichester, UK, 2012).

[22] Winberg, S. & Sneddon, L. Impact of intraspecific variation in teleost fishes: aggression, dominance status and stress physiology. Journal of Experimental Biology **225**, jeb169250 (2022). URL https://journals.biologists.com/jeb/article/225/20/jeb169250/278485/Impact-of-intraspecific-variation-in-teleost.

[23] Mushtaq, S. T. Aggression in aquatic environments and its relevance in aquaculture and conservation efforts. Discover Animals **1**, 28 (2024). URL https://link.springer.com/10.1007/s44338-024-00026-x.

[24] The State of World Fisheries and Aquaculture 2026 (FAO, 2026). URL https://openknowledge.fao.org/handle/20.500.14283/cd8357en.

[25] Kasumyan, A. O. & Pavlov, D. S. Problems and Prospects of Studying Schooling Behavior of Fish. Journal of Ichthyology **63**, 1393–1400 (2023). URL https://link.springer.com/10.1134/S0032945223070159.

[26] Schar, D., Klein, E. Y., Laxminarayan, R., Gilbert, M. & Van Boeckel, T. P. Global trends in antimicrobial use in aquaculture. Scientific reports **10**, 21878 (2020).

[27] Urbina, I. The dirty secret behind the farmed fish you eat. The New York Times Magazine (2026). URL https://www.nytimes.com/interactive/2026/10/08/magazine/farm-raised-fish-aquaculture-overfishing.html.

[28] Daskalova, A. Farmed fish welfare: stress, post-mortem muscle metabolism, and stress-related meat quality changes. International Aquatic Research **11**, 113–124 (2019). URL http://link.springer.com/10.1007/s40071-019-0230-0.

[29] Vicsek, T., Czirok, A., Ben-Jacobs, E., Cohen, I. & Shochet, O. Novel type of phase transition in a system of self-driven particles. Physical Review Letters **75**, 1226–1229 (1995).

[30] Couzin, I., Krause, J., James, R., Ruxton, G. & Franks, N. Collective memory and spatial sorting in animal groups. Journal of Theoretical Biology **2018**, 1–11 (2002).

[31] Cucker, F. & Smale, S. Emergent Behavior in Flocks. IEEE Transactions on Automatic Control **52**, 852–862 (2007).

[32] Kolpas, A. et al. How the Spatial Position of Individuals Affects Their Influence on Swarms: A Numerical Comparison of Two Popular Swarm Dynamics Models. PLoS ONE **8**, e58525 (2013). URL https://dx.plos.org/10.1371/journal.pone.0058525.

[33] Costanzo, A. & Hemelrijk, C. K. Spontaneous emergence of milling (vortex state) in a Vicsek-like model. Journal of Physics D: Applied Physics **51**, 134004 (2018). URL https://iopscience.iop.org/article/10.1088/1361-6463/aab0d4.

[34] Costanzo, A. Milling-induction and milling-destruction in a Vicsek-like binary-mixture model. EPL (Europhysics Letters) **125**, 20008 (2019). URL https://iopscience.iop.org/article/10.1209/0295-5075/125/20008.

[35] Klamser, P. P. et al. Impact of variable speed on collective movement of animal groups. Frontiers in Physics **9**, 715996 (2021).

[36] Szwaykowska, K., Romero, L. M.-y.-T. & Schwartz, I. B. Collective motions of heterogeneous swarms. IEEE Transactions on Automation Science and Engineering **12**, 810–818 (2015).

[37] Zhou, Y., Wang, T., Lei, X. & Peng, X. Collective behavior of self-propelled particles with heterogeneity in both dynamics and delays. Chaos, Solitons & Fractals **180**, 114596 (2024). URL https://linkinghub.elsevier.com/retrieve/pii/S0960077924001474.

[38] Zhang, J., Wang, W.-Y., Du, W.-B. & Cao, X.-B. Evolution of cooperation among mobile agents with heterogenous view radii.

Physica A: Statistical Mechanics and its Applications **390**, 2251–2257 (2011). URL https://linkinghub.elsevier.com/retrieve/pii/S0378437111001634.

[39] Copenhagen, K., Quint, D. A. & Gopinathan, A. Self-organized sorting limits behavioral variability in swarms. Scientific Reports **6**, 31808 (2016). URL https://www.nature.com/articles/srep31808.

[40] del Mar Delgado, M. et al. The importance of individual variation in the dynamics of animal collective movements. Philosophical Transactions of the Royal Society B: Biological Sciences **373**, 20170008 (2018).

[41] Ohira, T. Collective behaviors emerging from chases and escapes. Artificial Life and Robotics **29**, 1–11 (2024). URL https://link.springer.com/10.1007/s10015-023-00928-1.

[42] Colavecchia, M., Katopodis, C., Goosney, R., Scruton, D. A. & McKinley, R. S. Measurement of burst swimming performance in wild Atlantic salmon (Salmo salar L.) using digital telemetry. Regulated Rivers: Research & Management **14**, 41–51 (1998). URL https://onlinelibrary.wiley.com/doi/10.1002/(SICI)1099-1646(199801/02)14:1⟨41::AID-RRR475⟩3.0.CO;2-8.

[43] Grilli, F., Tokić, G. & Yue, D. K. Effects of induced behaviour on vortex formation and stability in swarms. Swarm Intelligence **20**, 1–26 (2026).

[44] Videler, J. J. Fish swimming Vol. 10 (Springer Science & Business Media, 1993).

[45] Tokić, G. & Yue, D. K. Optimal shape and motion of undulatory swimming organisms. Proceedings of the Royal Society B: Biological Sciences **279**, 3065 (2012).

[46] Tokić, G. & Yue, D. K. Energetics of optimal undulatory swimming organisms. PLOS Computational Biology **15**, e1007387 (2019).

[47] Wood, C., Turner, J. & Graham, M. Why do fish die after severe exercise? Journal of Fish Biology **22**, 189–201 (1983).

[48] Holder, P. E. et al. Are we any closer to understanding why fish can die after severe exercise? Fish and Fisheries **23**, 1400–1417 (2022).

[49] Rome, L. C., Swank, D. & Corda, D. How fish power swimming. Science **261**, 340–343 (1993).

[50] Rome, L. C. et al. Why animals have different muscle fibre types. Nature **335**, 824–827 (1988).